JOURNAL OF VIROLOGY, Aug. 2009, p. 7391–7396 Vol. 83, No. 15
0022-538X/09/$08.00+0 doi:10.1128/JVI.00479-09

Complete Virion Assembly with Scaffolding Proteins Altered in the Ability To Perform a Critical Conformational Switch▽

James E. Cherwa, Jr., and Bentley A. Fane*

Department of Plant Sciences and BIO5 Institute, University of Arizona, Tucson, Arizona 85719

Received 6 March 2009/Accepted 18 May 2009

In the ϕX174 procapsid, 240 external scaffolding proteins form a nonquasiequivalent lattice. To achieve this arrangement, the four structurally unique subunits must undergo position-dependent conformational switches. One switch is mediated by glycine residue 61, which allows a 30° kink to form in α-helix 3 in two subunits, whereas the helix is straight in the other two subunits. No other amino acid should be able to produce a bend of this magnitude. Accordingly, all substitutions for G61 are nonviable but mutant proteins differ vis-à-vis recessive and dominant phenotypes. As previously reported, amino acid substitutions with side chains larger than valine confer dominant lethal phenotypes. Alone, these mutant proteins appear to have little or no biological activity but rather require the wild-type protein to interact with other structural proteins. Proteins with conservative substitutions for G61, serine and alanine, have now been characterized. Unlike the dominant lethal proteins, these proteins do not require wild-type subunits to interact with other viral proteins and cause assembly defects reminiscent of those conferred by the lethal dominant proteins in concert with wild-type subunits. Although atomic structures suggest that only a glycine residue can provide the proper torsion angle for assembly, mutants that can productively utilize the altered external scaffolding proteins were isolated, and the mutations were mapped to the coat and internal scaffolding proteins. Thus, the ability to isolate strains that could utilize the single mutant D protein species would not have been predicted from past structural analyses.

Proper virion assembly requires a series of precise protein-protein interactions that proceed along an ordered morphogenetic pathway. During T=1 *Microvirus* assembly (canonical species: ϕX174, G4, and α3), early intermediates are directed into larger macromolecular structures by a class of transiently associated proteins called scaffolding proteins. These proteins mediate the conformational switching of structural proteins, assist in lowering the nucleation barrier for assembly, and ensure morphogenetic fidelity (10). While many large DNA viruses rely on a single internal scaffolding protein, the small microviruses and the satellite P4-like viruses require both internal and external scaffolding proteins (7, 11, 20). The atomic structures of the ϕX174 virion, procapsid, and assembly naïve external scaffolding protein have been determined by crystallography (5, 6, 14–16). Thus, biochemical and genetic data can be interpreted within a defined structural context.

The morphogenetic roles of the ϕX174 internal and external scaffolding proteins are illustrated in Fig. 1A. The first identifiable assembly intermediates are pentamers of the viral coat F and major spike G proteins; the respective 9S and 6S particles, which form independently of both scaffolding proteins (21). Five internal scaffolding B proteins bind to the underside of the 9S particle, yielding the 9S* intermediate (3). This interaction also induces a conformational change that allows 9S*-6S particle associations, forming the 12S* intermediate (19), which also contains the DNA pilot protein H (3). Twenty external scaffolding D proteins, most likely in the form of five tetramers or 10 asymmetric dimers (16), interact with the 12S* particle. D-D contacts mediate the construction of the procapsid (108S), an immature virus particle, presumably by allowing pentamers to interact across twofold axes of symmetry (1, 5, 6).

In the atomic structure of the viral procapsid (5, 6), there are four structurally distinct external scaffolding proteins (D_1 to D_4), arranged as dimers of dimers (D_1D_2, D_3D_4), per viral coat protein (Fig. 1B and C). As this unique arrangement bears no resemblance to a T=4 quasiequivalent structure, the external scaffolding protein must exist in two major conformations to accommodate the various D-D interactions required for lattice formation. One monomer in each asymmetric dimer, D_1 and D_3, must be bent 30°. This critical kink occurs at glycine residue 61 (G61) in α-helix 3 (Fig. 1C) and is also present in the crystal structure of the assembly naïve dimer D_AD_B (16). The organization of the genome further emphasizes the evolutionary importance of maintaining the G61 residue in the external scaffolding protein. Gene E, which encodes the lysis protein, resides entirely within the gene D sequence. Both proteins are translated from the same mRNA, and the G61 and gene E start codons overlap (18).

Theoretically, substitutions for G61 should inhibit the formation of the kinked conformer or alter its structure by changing the magnitude of the bend found in α-helix 3. As previously reported (3), proteins with substitutions for G61 were expressed from cloned genes under *lac* induction. The mutant proteins fell into two classes. G61-substituted amino acids with larger side chains (V, D, P, K) strongly inhibited wild-type ϕX174 morphogenesis, whereas the expression of proteins with smaller side chains (serine, alanine, and threonine, to be referred to as G61S, G61A, and G61T, respectively) did not affect wild-type ϕX174 assembly on the level of plaque formation. The G61S and G61T proteins were unable to complement a *nullD* mutant. Although the G61A protein did display some

* Corresponding author. Mailing address: The BIO5 Institute, Keating Building, University of Arizona, Tucson, AZ 85719. Phone: (520) 626-6634. Fax: (520) 621-6366. E-mail: bfane@u.arizona.edu.

▽ Published ahead of print on 27 May 2009.

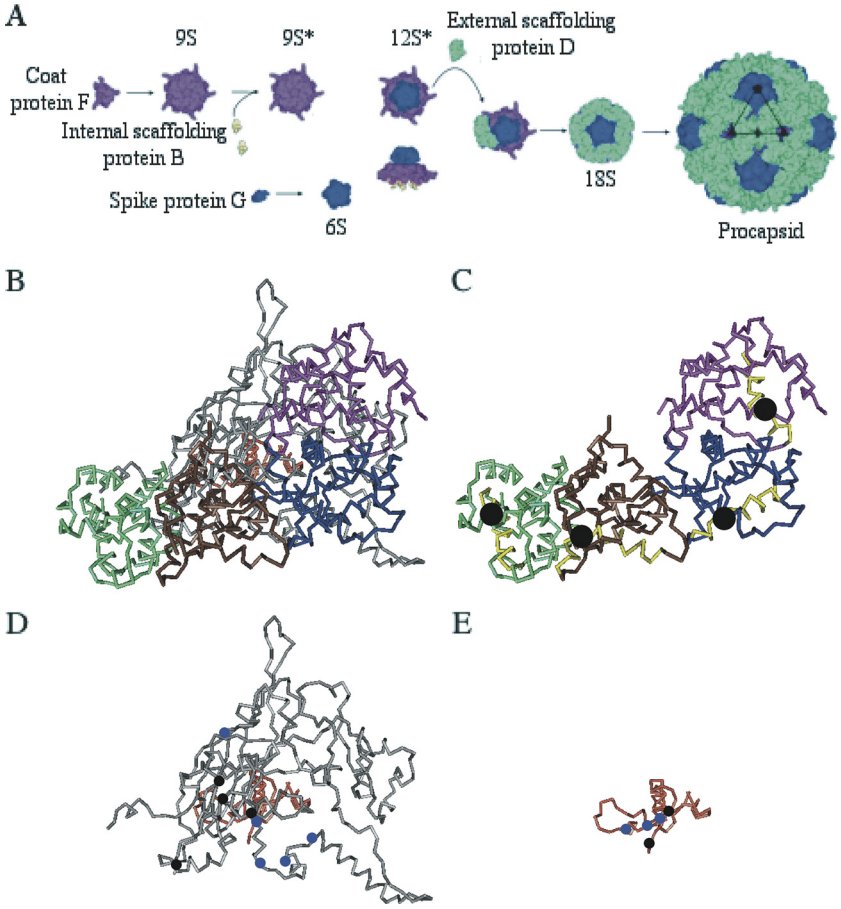

FIG. 1. (A) The ϕX174 procapsid assembly pathway. (B) External scaffolding subunits D_1 (purple), D_2 (blue), D_3 (brown), and D_4 (green); the coat protein (gray); and the internal scaffolding protein (peach) in the asymmetric unit. (C) The four external scaffolding proteins. The position of glycine residue 61 within α-helix 3, which is highlighted in yellow, is indicated by a black dot. (D) The locations of the *utilizer* (black dot) and resistance (blue dot) mutations (3) in the coat protein. Amino acid F426 is not depicted, as the very C terminus of the coat protein is unordered in the atomic structure (14, 15). (E) The locations of the *utilizer* (black dot) and resistance (blue dot) mutations in the internal scaffolding protein. Amino acid B2 is not depicted, as the N terminus of the internal scaffolding protein is unordered in the procapsid atomic structure (5, 6). The structures in panels B, C, D, and E are rendered at the same scale and in the same orientation.

complementation activity, it was extremely weak and was only observed at 42°C.

The previous studies focused on the dominant lethal proteins, those with substituted side chains of valine or larger. Alone in *nullD* infections, these mutant proteins displayed no activity vis-à-vis their ability to interact with other viral proteins. Assembly was arrested after the formation of the 12S* particle, the last intermediate before the requirement of the external scaffolding protein (Fig. 1A). However, in wild-type infections, in which both the wild-type and mutant proteins were present, early assembly intermediates were removed from the pathway. Thus, mutant–wild-type heterodimers are the inhibitory species. In the present study, the behavior of the G61S, G61A, and G61T proteins was investigated. Unlike the previously characterized proteins, the G61S and G61A proteins appear to interact with other viral proteins and/or early assembly intermediates in the absence of the wild-type subunit, suggesting that mutant homodimers retain some level of function. To further test this hypothesis, ϕX174 mutants that could exclusively utilize these mutant proteins to produce viable progeny were isolated. The torsional angle necessary for the D protein to properly adopt one of its two conformations can only be accommodated by a glycine residue, as the other amino acid side chains occupy forbidden regions of the Ramachandran plot. Thus, the ability to isolate strains that could utilize the single mutant D protein species would not have been predicted from past structural analyses.

MATERIALS AND METHODS

Phage plating, media, buffers, and stock preparation. The reagents, media, buffers, and protocols used in this study have been previously described (8).

Bacterial strains, phage strains, and plasmids. *Escherichia coli* C strains C122 (*sup*°) and BAF30 (*recA*) have been previously described (8, 9). The host *slyD* mutation confers resistance to E protein-mediated lysis (17). The ϕX174 *nullD* mutant and the complementing plasmid pϕXDJ have been previously reported (2). The construction of cloned D genes with substitutions for glycine 61 has been previously described (3). Plasmid names reflect the expressed mutant protein. For example, pG61S refers to a plasmid encoding a ϕX174 D protein with a glycine-to-serine substitution at amino acid 61. Likewise, G61S refers to the mutant D protein expressed from the plasmid.

Isolation of *utilizer* mutants. ϕX174 *nullD* was plated on cells expressing the mutated protein, i.e., BAF30/pG61A, BAF30/pG61S, and BAF30/pG61T. Plates were incubated at 37°C until plaques appeared. Phage from the plaques were transferred to three indicator lawns seeded with the wild-type host C122, BAF30/

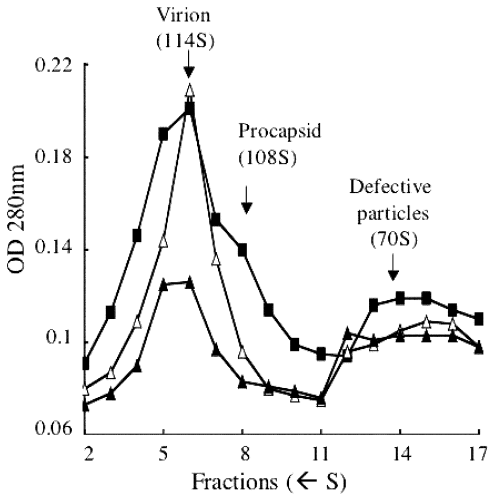

FIG. 2. Large particles synthesized in wild-type-infected cells. Symbols: closed squares, no inhibitory protein expression; open triangles, low induction of the G61S protein; closed triangles, high induction of the G61S protein. See text for the definition of low- and high-induction conditions.

pφXDJ, and a host expressing the mutant external scaffolding protein used in the selection. *utilizer* mutants were identified by the retention of the complementation-dependent phenotype. Putative mutants were plaque purified, and subsequent plating assays were performed to confirm that the phenotype bred true.

In vivo characterization of the morphogenetic pathway and the kinetics of virus production. Extracts of lysis-resistant infected cells were generated and processed as previously described (3). Virions and assembly intermediates were separated by rate-zonal sedimentation. Extract samples were loaded atop a 5 to 30% sucrose gradient in 13-by-51-mm tubes and subjected to ultracentrifugation in a Beckman SW55 Ti rotor at 45,000 rpm for 1.0 h at 18°C. After gradient fractionation, UV spectrophotometry (optical density at 280 nm [OD_{280}]) was used to detect particles with S values larger than 70. Sodium dodecyl sulfate-polyacrylamide gel electrophoresis (SDS-PAGE) of gradient fractions was used to detect particles with S values of less than 50. The protocols used to examine the kinetics of virion production have been previously described (22).

RESULTS

Biochemical analysis of particles produced by the external scaffolding proteins with conservative G61 substitutions. The results of a previous analysis (3) indicated that the expression of dominant lethal external scaffolding proteins conferred an early and very strong block in assembly. The amino acids substituted for G61 had side chains larger than valine. The expression of proteins with more-conservative substitutions (S, A, and T) produced modest decreases in burst and plaque size. These reductions could result from a decrease in assembly efficiency or the production of noninfectious assembled particles. To distinguish between these two alternatives, the large particles produced in wild-type-infected cells expressing the G61S, G61A, and G61T proteins were characterized. The concentration of the isopropyl-β-D-thiogalactopyranoside (IPTG) inducer used in these experiments yields a wild-type-to-mutant D protein ratio of approximately 1:1 (22). After the removal of unabsorbed virions, incubation, and chemical lysis, soluble material was subjected to rate-zonal sedimentation. Following centrifugation, samples were separated into approximately 50 0.1-ml fractions. Particles, regardless of infectivity, were detected by UV spectroscopy at 280 nm.

As shown in the sedimentation profiles in Fig. 2, wild-type yields were decreased in cells expressing the G61S protein. Yield reduction was proportional to the induction level of the cloned gene. Although low levels of defective particles, which sediment at 70S, were detected in all extracts, their relative levels were roughly proportional to the yield of virions. To determine whether the particles that sediment at 114S were as infectious as the particles produced in the control infection, the specific infectivity values (PFU/OD_{280}) were calculated. No significant differences were observed between the particles isolated from the various infections; typical specific infectivity values were approximately 9.0×10^{11} PFU/OD_{280} and did not vary by more than a factor of 2.0 in this and other experiments. These results suggest that the expression of the mutant proteins most likely affect the efficiency of particle formation. Similar results were obtained with cells expressing the G61T protein (data not shown). The G61A protein is discussed below. Although the early assembly intermediates were also characterized, the block in assembly was too modest to reliably determine which assembly step was inhibited. Thus, further characterizations focused on analyzing the activity of the mutant proteins in the absence of the wild-type subunit.

As previously reported, the lethal dominant D proteins having G61 substitutions with side chains larger than valine only displayed activity in the presence of the wild-type D protein. Alone, these mutant proteins behaved as if there were no D protein present (3). The G61A protein very weakly complemented a *nullD* mutant at 42°C (Table 1), while the G61S and G61T proteins displayed no complementation activity. To further characterize the activity of these two proteins, extracts of *nullD* mutant-infected cells were generated and examined as described above. No large particles were observed (data not

TABLE 1. Plating efficiency[a] of φX174 WT, *nullD*, and *ut3d*/*nullD* strains

Strain[c]	Substitution for G61[b]			
	WT	S	A	T
WT	1.0	1.0	1.0	1.0
nullD	1.0	RF[d]	RF	RF
nullD at 42°C[e]	1.0	RF	0.6	RF
ut3d(B)H109Y/nullD	1.0	0.9	0.7	RF
ut3d(B)Q2H/nullD	1.0	0.2	0.4	RF
ut3d(F)E42Y/nullD	1.0	0.6	1.0	RF
ut3d(F)S426L/nullD	1.0	0.8	1.0	RF
ut3d(F)T144A/nullD	1.0	RF	0.7	RF
ut3d(F)Y70H/nullD	1.0	RF	1.0	RF
ut3d(F)D87G/nullD	1.0	RF	0.4	RF

[a] Plating efficiency = titer on a cell line expressing a mutant external scaffolding protein/titer on a cell line expressing the wild-type (WT) external scaffolding protein.

[b] The protein expressed in the cell: WT, wild-type protein; S, glycine 61→serine mutant protein; A, glycine 61→alanine mutant protein; T, glycine 61→threonine mutant protein.

[c] Mutant names reflect conferred amino acid substitutions. For example, *ut3d(B)H109Y* represents *utilizer* of mutant α-helix 3 D protein with a change in internal scaffolding protein B, histidine 109→tyrosine.

[d] RF, am^+ reversion frequency of the *nullD* strain, which contains two adjacent amber mutations. The am^+ reversion frequencies ranged from 10^{-4} to 10^{-6}, depending on the *nullD* mutant stock used in the experiment.

[e] The Gl61A protein could weakly complement the *nullD* mutant at 42°C. Although the plating efficiency was high and reproducible, the plaque size was extremely small. All of the other data shown were generated at 37°C. No other temperature-dependent phenotypes were observed.

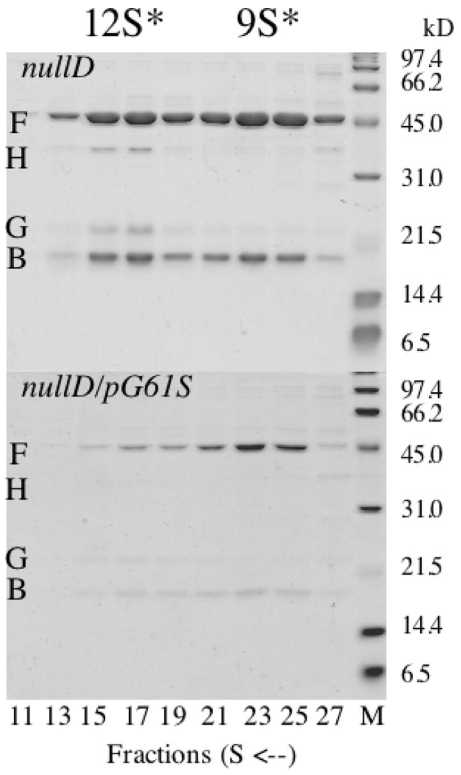

FIG. 3. Analysis of early assembly intermediates synthesized in *nullD* mutant-infected cells. For these experiments, each gradient was prepared as described in Materials and Methods and separated into approximately 50 80-μl fractions. Every other fraction was analyzed by 15% SDS-PAGE. Only the relevant fractions are depicted, i.e., fractions 11 to 27 from the bottom of the tube. The 12S* particle is located in fractions 15 to 17, and the 9S* particle is shown in fractions 23 to 25. The lane at the far right contains a molecular weight marker. Viral proteins are labeled as followed: F, coat protein; H, minor spike protein; G, major spike protein; B, internal scaffolding protein.

shown). To characterize the early assembly intermediates, after rate-zonal sedimentation, fractions were analyzed by SDS-PAGE. The *nullD* control infection, in which no external scaffolding protein is present, resulted in the accumulation of the 12S* particle, containing the major capsid F, spike G, internal scaffolding B, and DNA pilot H proteins (Fig. 3). This result is consistent with the sequential order of protein interactions in the assembly pathway (Fig. 1A), as the 12S* particle is the last assembly intermediate prior to the D protein's entering morphogenesis. In contrast, *nullD* mutant infection of cells expressing the mutant G61S external scaffolding protein resulted in skewing toward the recovery of the 9S* particle compared to that in the *nullD* mutant control (Fig. 3). The ratio of coat protein found in 9S* and 12S* particles was determined by using Image J software. For the infection of cells expressing the G61S protein, the ratio was approximately 3:1, whereas the ratio was approximately 1:1 in the *nullD* mutant control infection. This result is reminiscent of those previously obtained with heterodimers of the wild-type and lethal dominant external scaffolding proteins (3). Thus, the prevalence of the 9S* particle when only the G61S protein is present may indicate that G61S homodimers, like wild-type–lethal dominant heterodimers, are able to enter morphogenesis and remove 12S* particles from the productive pathway. Results obtained from *nullD* mutant infections of cells expressing the G61T protein were similar to those observed with the *nullD* mutant control, suggesting that this protein alone lacks the ability to interact with other phage proteins (data not shown).

Isolation of *utilizer* mutants. Although the results of the biochemical analysis are suggestive, a more compelling case for mutant protein activity could be made if full complementation could be achieved. Toward this end, viral mutants that could exclusively utilize the G61S or G61A external scaffolding protein were isolated via direct genetic selection. To ensure a wide array of independently isolated genotypically different mutations (13), nine ϕX174 *nullD* stocks were plated with cells expressing each mutant protein and incubated at 37°C. *utilizer* mutants were identified by their ability to form plaques on cells expressing an exogenous mutant D protein while retaining a complementation-dependent phenotype. The entire genomes of two mutants, *ut3d*(*F*)*S426L*/*nullD* and *ut3d*(*B*)*H109*Y/*nullD*, were sequenced and compared to that of the wild type; no other nucleotide changes were observed, indicating that the reported substitutions are both necessary and sufficient to confer the *utilizer* phenotype. The efficiency-of-plating value of each *utilizer* mutant was comparable to that of the wild-type control (Table 1); however, plaque sizes were observably smaller in each case. Typically, the plaque diameter of any *nullD*/*utilizer* mutant strain on cells expressing the G61A protein was half of that observed on cells expressing the wild-type protein, which did not differ significantly from the *nullD* parental strain. *nullD*/*utilizer* plaque morphology was further reduced on cells expressing the G61S protein. All of the isolated mutations confer the ability to utilize the G61A protein; however, only a subset of the mutations confers the utilization of the G61S protein. As an alanine substitution is more conservative, it follows that a wider array of *utilizer* mutations would be active with the G61A protein.

Several attempts were made to isolate a mutant that could utilize the G61T external scaffolding protein. If such a genotype exists, it occurs at a frequency of $<10^{-8}$, which indicates that multiple mutational events may be required. Therefore, the *ut3d*(*B*)*H109Y*/*nullD* strain, which forms plaques on cells expressing both the G61S and G61A proteins, was used in an effort to isolate the mutant. Once again, no mutants were recovered above a frequency of 10^{-8}. Therefore the threonine substitution may represent the threshold of side chain length, atomic volume, and surface area tolerated for productive assembly (4, 23).

Kinetics of assembly suggest a delay in nucleation. To further characterize the *utilizer* mutants, the in vivo kinetics of virion production was investigated. Lysis-resistant cells expressing the wild-type and G61S proteins were infected at a low multiplicity of infection with either the *nullD* or the *ut3d*(*B*)*H109Y*/*nullD* mutant strain. In these experiments, virions were preattached and the infections were synchronized as previously described (22). At each time point, cells were chemically lysed and samples were plated to determine viral titers. As shown in Fig. 4, the exponential phase for the *utilizer* viral cycle was delayed in cells expressing the G61S protein (closed triangles) compared to that of cells expressing the wild-type protein (open circles). The extended lag phase most likely represents a delay in procapsid nucleation. Afterward, the rate

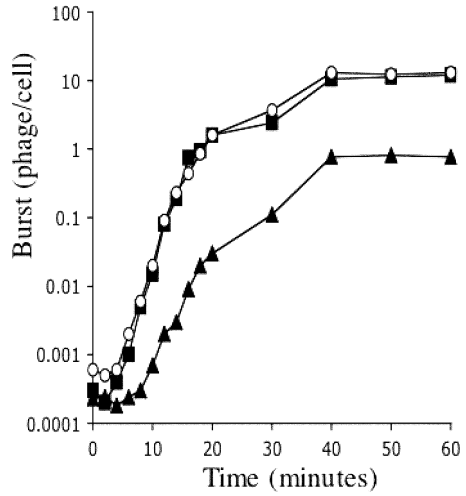

FIG. 4. Kinetics of phage growth presented as burst (phage number per cell). Infections were conducted in lysis-resistant cells, and aliquots were removed every 2 min for the first 20 min and every 10 min thereafter. Symbols: closed squares, *nullD* mutant infection of cells expressing the cloned wild-type D protein; open circles, *ut3d(B)H109Y/nullD* mutant infection of cells expressing the cloned wild-type D protein; closed triangles, *ut3d(B)H109Y/nullD* mutant infection of cells expressing the G61S protein.

of virion production may also be decreased, which may reflect slower elongation reactions. Similar results were observed with the expression of the G61A protein (data not shown).

DISCUSSION

As evinced by the results of structural, biochemical, and genetic analyses (3, 5, 16), the conformational switch mediated by glycine residue 61 of the ϕX174 external scaffolding protein is critical for proper assembly. The switch allows α-helix 3 to assume one of two conformations, straight or kinked, depending on the position of the subunit within either the external scaffolding protein lattice or the assembly naïve asymmetric dimer. The expression of cloned D genes with G61 missense mutations conferred two phenotypes (3). Substitutions with large side chains (V, D, K, P) inhibited wild-type plaque formation, a dominant lethal phenotype, whereas more-conservative amino acid substitutions (S, A, T) appear to be recessive vis-à-vis the ability to inhibit wild-type plaque formation. In the absence of the wild-type D protein, the dominant lethal proteins do not appear to enter the morphogenetic pathway. The last intermediate before the requirement of functional D protein, the 12S* particle, accumulates in *nullD* mutant-infected cells. However, in the presence of the wild-type D protein, 12S* particles appear to be removed from the assembly pathway, suggesting that the inhibitory species is a heterodimer consisting of mutant and wild-type subunits (3).

In this report, the effects of the D proteins with conservative substitutions for G61 (S, A, T) were analyzed both in the presence and in the absence of the wild-type protein. Like the dominant lethal proteins, the G61S and G61T proteins were unable to complement a *nullD* mutant. The G61A protein exhibited weak complementation but only at 42°C. In *nullD* mutant-infected cells expressing any of these three proteins at 37°C, large particles, i.e., procapsids, defective procapsids, or noninfectious particles, were not detected. Although the 12S* particle was detected, it was not the predominant assembly intermediate in cells expressing the G61S protein. The recovery of early assembly intermediates was skewed toward the 9S* intermediate, which precedes the 12S* particle in morphogenesis. This result suggests that the protein may have some activity in the absence of the wild-type subunit vis-à-vis the ability to interact with other phage components.

To test this hypothesis, an attempt was made to isolate ϕX174 *nullD* mutants that could form infectious progeny with only altered D proteins. Unlike previous attempts conducted with the dominant lethal proteins, mutants capable of exclusively utilizing the G61S and G61A proteins could be isolated. However, no single or double mutants capable of utilizing the G61T protein were recovered, substantiating the hypothesis that the mutational tolerance at the G61 site is a function of the substituted amino acid side chain size. Neither the ability to isolate *utilizer* mutations nor the weak complementation by the G61A protein would have been predicted from the atomic structure of the assembly naïve dimer. Only a glycine residue allows the proper kinked conformation, as the required torsion angles for other amino acids occupy forbidden regions of the Ramachandran plot (16). Thus, the full thermodynamic variability, flexibility, and tolerance of a protein or system to mutational and evolutionary manipulation are not entirely apparent in X-ray structures.

The serine-to-leucine *utilizer* mutation at amino acid 426 of the coat F protein was also isolated as a mutation that conferred resistance to the inhibitory heterodimers in the previous study (3), suggesting that the two phenomena may be related. Furthermore, both mutation types, which map to either the viral coat F or the internal scaffolding B protein, cluster beneath either the D_3 subunit or the D_2-D_3 interface (Fig. 1B to E) in the atomic structure of the "closed" procapsid (5, 6). The closed procapsid most likely represents an off-pathway product having undergone a maturation event during crystallization. In the cryoelectron microscopy reconstruction of the "open" procapsid, which most likely represents the native species, there are 30-Å pores at the threefold axes of symmetry (1, 12). Thus, the coat protein helices, in which some of the mutations reside, would most likely be shifted upward toward the center of the asymmetric unit, occupying a region under the D_2 and D_3 subunits.

The atomic structures of *utilizer* procapsids and the mutant external scaffolding proteins have not been solved. Therefore, the exact structural changes imposed upon the external scaffolding lattice remain unknown. However, dramatic alterations would be required to place the *utilizer* or previously isolated *resistant* mutants in direct contact with the mutated G61 residues. The viral coat protein physically separates the internal and external scaffolding proteins, thus blocking direct contacts between the affected amino acids in the two scaffolding proteins. The coat protein *utilizer* mutations can make direct contact with the D_2 and D_3 external scaffolding protein subunit, but these interactions are with the subunits' undersides, whereas the altered G61 residue is most likely surface exposed. Thus, the coat protein *utilizer* mutations most likely alter the outer surface of the coat protein to facilitate assembly with the mutant scaffolding proteins. These requisite alterations can

also be stimulated by coat-internal scaffolding protein interactions, which are important in producing conformational changes that allow the 9S* intermediate to interact with other phage proteins (Fig. 1A).

The results of kinetic experiments indicate that acquisition of the *utilizer* mutation does not appear to affect the kinetics of assembly with the wild-type protein (Fig. 4, open circles and closed squares, respectively). However, an extended lag phase was observed with the G61S and G61A mutant species (Fig. 4, closed triangles). There is no temporal gene expression in the ϕX174 system; therefore, the extended lag phase most likely reflects a delay in procapsid nucleation. As few or no coat-coat protein contacts are observed in the viral procapsid (1), the nucleation reaction is most likely mediated by D proteins interacting across twofold axes of symmetry. Many of these interactions are coordinated by amino acids in α-helix 3 of the D_2 and D_3 subunits, in which the wild-type G61 residue also resides. Thus, substitutions for G61 may alter hydrogen bonds or electrostatic interactions across twofold axes of symmetry. In turn, the *utilizer* mutations may restore interactions by altering the position of the overall lattice. For example, the *utilizer* mutation at amino acid 144 in the viral coat protein eliminates known coat-D_2 protein contacts, perhaps providing the flexibility necessary for the D_2 subunits to interact with adjacent D proteins across the twofold axes of symmetry in an altered lattice.

Even during wild-type assembly, off-pathway products are produced. However, the complex equilibria between possible nucleation reactions favor procapsid assembly, as opposed to off-pathway products. Missense mutations of G61 most likely prevent D proteins from interacting across the twofold axis of symmetry in a manner consistent with nucleating procapsid assembly. In turn, this skews the equilibria of nucleation reactions toward an off-pathway reaction that removes 12S* particles from productive morphogenesis. These off-pathway reactions are more effectively mediated by G61S and G61A homodimers, as well as wild-type–lethal dominant heterodimers. The *utilizer* mutations, as with the previously identified resistance mutations, most likely shift the balance toward productive assembly by either lowering the thermodynamic barrier for procapsid assembly or elevating the thermodynamic barrier of the off-pathway reactions. As it is very difficult to physically separate nucleation from elongation reactions, it is possible that off-pathway reactions could follow nucleation, conferring a defect early in elongation.

ACKNOWLEDGMENTS

We thank Barbara Vona for manuscript assistance.

This research was supported by National Science Foundation grant MCB 054297 to B.A.F. and an NSF Graduate Research Fellowship to J.E.C.

REFERENCES

1. **Bernal, R. A., S. Hafenstein, N. H. Olson, V. D. Bowman, P. R. Chipman, T. S. Baker, B. A. Fane, and M. G. Rossmann.** 2003. Structural studies of bacteriophage alpha3 assembly. J. Mol. Biol. **325:**11–24.
2. **Burch, A. D., and B. A. Fane.** 2000. Foreign and chimeric external scaffolding proteins as inhibitors of *Microviridae* morphogenesis. J. Virol. **74:**9347–9352.
3. **Cherwa, J. E., Jr., A. Uchiyama, and B. A. Fane.** 2008. Scaffolding proteins altered in the ability to perform a conformational switch confer dominant lethal assembly defects. J. Virol. **82:**5774–5780.
4. **Chothia, C.** 1975. Structural invariants in protein folding. Nature **254:**304–308.
5. **Dokland, T., R. A. Bernal, A. Burch, S. Pletnev, B. A. Fane, and M. G. Rossmann.** 1999. The role of scaffolding proteins in the assembly of the small, single-stranded DNA virus phiX174. J. Mol. Biol. **288:**595–608.
6. **Dokland, T., R. McKenna, L. L. Ilag, B. R. Bowman, N. L. Incardona, B. A. Fane, and M. G. Rossmann.** 1997. Structure of a viral procapsid with molecular scaffolding. Nature **389:**308–313.
7. **Fane, B. A., K. L. Brentlinger, A. D. Burch, S. L. Hafenstein, E. Moore, C. R. Novak, and A. Uchiyama.** 2006. ϕX174 et al., p. 129–145. *In* R. Calendar (ed.), The bacteriophages, second ed. Oxford Press, London, United Kingdom.
8. **Fane, B. A., and M. Hayashi.** 1991. Second-site suppressors of a cold-sensitive prohead accessory protein of bacteriophage ΦX174. Genetics **128:** 663–671.
9. **Fane, B. A., S. Head, and M. Hayashi.** 1992. Functional relationship between the J proteins of bacteriophages ϕX174 and G4 during phage morphogenesis. J. Bacteriol. **174:**2717–2719.
10. **Fane, B. A., and P. E. Prevelige, Jr.** 2003. Mechanism of scaffolding-assisted viral assembly. Adv. Protein Chem. **64:**259–299.
11. **Goldstein, R., J. Lengyel, G. Pruss, K. Barrett, R. Calendar, and E. Six.** 1974. Head size determination and the morphogenesis of satellite phage P4. Curr. Top. Microbiol. Immunol. **68:**59–75.
12. **Ilag, L. L., N. H. Olson, T. Dokland, C. L. Music, R. H. Cheng, Z. Bowen, R. McKenna, M. G. Rossmann, T. S. Baker, and N. L. Incardona.** 1995. DNA packaging intermediates of bacteriophage phi X174. Structure **3:**353–363.
13. **Luria, S. E., and M. Delbruck.** 1943. Mutations of bacteria from virus sensitivity to virus resistance. Genetics **28:**491–511.
14. **McKenna, R., L. L. Ilag, and M. G. Rossmann.** 1994. Analysis of the single-stranded DNA bacteriophage phi X174, refined at a resolution of 3.0 A. J. Mol. Biol. **237:**517–543.
15. **McKenna, R., D. Xia, P. Willingmann, L. L. Ilag, S. Krishnaswamy, M. G. Rossmann, N. H. Olson, T. S. Baker, and N. L. Incardona.** 1992. Atomic structure of single-stranded DNA bacteriophage phi X174 and its functional implications. Nature **355:**137–143.
16. **Morais, M. C., M. Fisher, S. Kanamaru, L. Przybyla, J. Burgner, B. A. Fane, and M. G. Rossmann.** 2004. Conformational switching by the scaffolding protein D directs the assembly of bacteriophage ϕX174. Mol. Cell **15:**991–997.
17. **Roof, W. D., H. Q. Fang, K. D. Young, J. Sun, and R. Young.** 1997. Mutational analysis of slyD, an Escherichia coli gene encoding a protein of the FKBP immunophilin family. Mol. Microbiol. **25:**1031–1046.
18. **Sanger, F., A. R. Coulson, T. Friedmann, G. M. Air, B. G. Barrell, N. L. Brown, J. C. Fiddes, C. A. Hutchison III, P. M. Slocombe, and M. Smith.** 1978. The nucleotide sequence of bacteriophage phiX174. J. Mol. Biol. **125:**225–246.
19. **Siden, E. J., and M. Hayashi.** 1974. Role of the gene beta-product in bacteriophage phi-X174 development. J. Mol. Biol. **89:**1–16.
20. **Six, E. W., M. G. Sunshine, J. Williams, E. Haggard-Ljungquist, and B. H. Lindqvist.** 1991. Morphopoietic switch mutations of bacteriophage P2. Virology **182:**34–46.
21. **Tonegawa, S., and M. Hayashi.** 1970. Intermediates in the assembly of phi X174. J. Mol. Biol. **48:**219–242.
22. **Uchiyama, A., and B. A. Fane.** 2005. Identification of an interacting coat-external scaffolding protein domain required for both the initiation of ϕX174 procapsid morphogenesis and the completion of DNA packaging. J. Virol. **79:**6751–6756.
23. **Zamyatnin, A. A.** 1972. Protein volume in solution. Prog. Biophys. Mol. Biol. **24:**107–123.